

Bolted connectors with mechanical coupler embedded in concrete: Shear resistance under static load

Ivan Milićević^{1a}, Branko Milosavljević^{*1}, Marko Pavlović^{2b} and Milan Spremić^{1c}

¹Faculty of Civil Engineering, University of Belgrade, Bulevar kralja Aleksandra 73, 11000 Belgrade, Serbia

²Faculty of Civil Engineering and Geosciences, Delft University of Technology, Stevinweg 1, Delft, CD, Netherlands

(Received May 3, 2019, Revised July 9, 2020, Accepted July 14, 2020)

Abstract. Contemporary design and construction of steel-concrete composite structures employs the use of prefabricated concrete elements and demountable shear connectors in order to reduce the construction time and costs and enable dismantling of elements for their potential reuse at the end of life of buildings. Bolted shear connector with mechanical coupler is presented in this paper. The connector is assembled from mechanical coupler and rebar anchor, embedded in concrete, and steel bolt, used for connecting steel to concrete members. The behaviour and ultimate resistance of bolted connector with mechanical coupler in wide and narrow members were analysed based on push-out tests and FE analyses conducted in Abaqus software, with focus on concrete edge breakout and bolt shear failure modes. The effect of concrete strength, concrete edge distance and diameter and strength of bolts on failure modes and shear resistance was analysed. It was demonstrated that premature failure by breakout of concrete edge occurs when connectors are located 100 mm or closer from the edge in low-strength and normal-strength reinforced concrete. Furthermore, the paper presents a relatively simple model for hand calculation of concrete edge breakout resistance when bolted connectors with mechanical coupler are used. The model is based on the modification of prediction model used for cast-in and post-installed anchors loaded parallel to the edge, by implementing equivalent influence length of connector with variable diameter. Good agreement with test and FE results was obtained, thus confirming the validity of the proposed method.

Keywords: steel-concrete composite structures; shear connectors; mechanical couplers; shear resistance; concrete edge breakout resistance; finite element analysis

1. Introduction

Composite structures formed by connecting steel and concrete elements have been competitive structural system in building and bridge construction around the world for a long time. The concept of combining steel and concrete elements within the same structure is based on utilizing the advantage of each widely used building material with aim to improve overall structural performance and to optimize the total costs of structures and structural components such as bridges, composite floors in high-rise buildings, braced RC frames, etc. The performance of steel-concrete composite structures in resisting external loads depends on the behaviour of the connection between reinforced concrete and steel members. Since steel-concrete connections are mostly loaded in longitudinal shear, their capacity and behaviour depend on shear strength and stiffness of applied type of shear connector.

Traditionally, shear connection of composite beams with

in-situ casted concrete slab is achieved by welding headed studs on the top flange of steel beam, continuously and uniformly along the beam length. The extensive use of this type of shear connector comes from rapid automatic welding procedure and excellent performance proved by comprehensive scientific research and building practice. Ollgaard *et al.* (1971) and Oehlers (1980) conducted a series of experimental tests to explain the behaviour of headed shear studs and the effect of influencing parameters on their bearing capacity. Very extensive state of the art was given by Pallarés and Hajjar (2010), based on the comparison of 391 test results of welded headed studs loaded in shear.

In past decades, an attempt to reduce the construction time and costs of steel-concrete composite structures was made by the prefabrication of concrete elements which can be interconnected by local in-situ concreting. Grouped arrangements of headed studs in precast composite decks are often used as an alternative for rigid block shear connectors, because of higher ductility and easier execution. Okada *et al.* (2006), Xu *et al.* (2012), Xue *et al.* (2012), Guezouli *et al.* (2013) and Yu-Hang *et al.* (2019) experimentally and numerically investigated the behaviour of grouped headed studs. The behaviour of several group arrangements and resistance of groups with closely spaced headed studs was analysed by (Spremić *et al.* 2013, Spremić *et al.* 2017, Spremić *et al.* 2018), with aim to reduce the dimensions of grouped headed studs and

*Corresponding author, Assistant Professor

E-mail: brankom@imk.grf.bg.ac.rs

^aTeaching Assistant, Ph.D. Student

E-mail: ivanm@imk.grf.bg.ac.rs

^bAssistant Professor

^cAssistant Professor

openings in precast concrete slabs.

Apart from reducing the construction time and costs, prefabrication of concrete elements is one of the steps towards more sustainable design and construction of steel-concrete composite structures and circular economy concept. In contrast to traditional composite structures with monolithic nature, the use of prefabricated concrete elements with bolted shear connectors enables relatively easy deconstruction and reuse of structural elements in the end-of-life scenario (Brambilla *et al.* 2019).

Several experimental and numerical studies of various types of demountable shear connectors have been conducted over the past decades, mostly by push-out tests and FE models. Among the first to investigate the possibility of application of bolts as shear connectors were Dallam (1968) and Marshall *et al.* (1971), who conducted a series of push-out tests on friction grip bolts. Recently, Liu *et al.* (2014) and Ataei *et al.* (2016) investigated the behaviour of composite beams with friction grip bolts and geopolymer precast concrete slabs, in order to improve their sustainability. Bolted shear connectors, which are intended to transfer full shear force through bearing on concrete and steel flange and shear in threaded part of the bolt, were analysed in different configurations: (1) without embedded nut by Hawkins (1987), (2) with single embedded nut by Dedic and Klaiber (1984), Lee and Bradford (2013) and (Pavlović *et al.* 2013; Pavlović and Veljković 2017), and (3) with double embedded nut by Schaap (2004) and Kwon (2008). It is shown that higher initial stiffness can be achieved by embedding nut in the concrete, which restrains the rotation of the bolt at steel-concrete surface. Demountable shear connectors in the form of headed stud shear connector was analysed by Dai *et al.* (2015) and Lam *et al.* (2017), with different details of the connection. It was demonstrated that demountable connectors have similar stiffness and higher ductility compared to welded headed studs while providing full ability to separate the slab for reuse. Pathirana *et al.* (2016) investigated blind bolts as demountable shear connectors and concluded that the behaviour of blind bolts is comparable to the behaviour of welded headed studs.

Grosser (2012) conducted research on cast-in and post-installed anchors loaded in shear under arbitrary direction. An extensive state of the art on existing experimental and numerical results on post installed anchors was given. As a result of comprehensive experimental study and nonlinear FE analysis, a new concept of generating and transferring local stresses in concrete for anchors loaded in shear was developed. In case of anchors loaded in shear parallel to the concrete edge and located near the edge, Grosser (2012) developed a relatively simple prediction model for hand calculation of concrete edge breakout resistance, which is based on the analogy with lateral blow-out failure of anchors loaded in tension and located near concrete edge. The proposed prediction model gives more accurate test-to-predicted resistance ratios compared to models given in different design codes. Dimensions of anchor i.e., diameter and embedment depth, concrete strength and concrete edge distance were designated as main parameters that affect concrete edge breakout resistance.

Bolted shear connector with mechanical coupler presented in this paper is made out of two main parts, as shown in Fig. 1. The first part consists of mechanical coupler and rebar anchor placed in formwork before concrete casting. After formwork removal, steel bolt is used to connect steel and concrete members, as a second part of the assembly. This type of shear connector can be used in building and bridge construction, with either cast in-situ or precast concrete, to ensure the reduction of construction time and enable easier dismantling for potential reuse at the end of life of buildings. Based on the layout presented in Fig. 1, bolted connectors with mechanical coupler have some performance advantages over connectors with constant diameter and limited embedment depth: diameter of mechanical coupler is larger than diameter of used bolt, thus providing larger bearing surface beneath the connector, while long rebar anchor eliminates the possibility of pryout and pullout failure modes. Therefore, the behaviour and shear resistance can be compared to that of bolted shear connectors with single or double embedded nut and post installed anchors with large embedment depth.

After a review of literature, it was found that published research work on bolted shear connectors with mechanical couplers is very limited. Yang *et al.* (2018) described the behaviour of bolted connectors assembled from the short bolt, mechanical coupler and the second (long) bolt, instead of rebar anchor shown in Fig. 1. All test specimens failed in bolt shear failure mode with insignificant concrete damage because high concrete strength was used. Shear resistance was approximately equal to corresponding welded stud connectors but with lower ductility in all cases. Milosavljević *et al.* (2018) described the performance of bolted connectors with mechanical coupler and rebar anchor, emphasizing the effect of distance between the connector and concrete edge on the type of failure mode in normal strength concrete. FE models in Abaqus were validated against experimental observations and used for detail description of concrete damages and distribution of internal forces in the connector in different failure modes.

Since there is lack of information about the behaviour of bolted connectors with mechanical coupler under static shear load, they are rarely used in construction practice and there is no guidance for their design in the literature. The main objective of this paper is to provide recommendations for design of bolted shear connectors with mechanical coupler. Two possible failure modes were analysed: bolt shear failure and concrete edge breakout failure mode. FE parametric study was performed to show more in-depth influence of concrete edge distance, concrete strength and bolt diameter on shear stiffness, resistance and ductility of the connection. Finally, the recommendations for minimum edge distance to avoid concrete edge failure are given.

2. Experimental research

The aim of experimental research was to investigate the behaviour of bolted connectors with mechanical coupler and rebar anchor embedded in concrete, used as shear

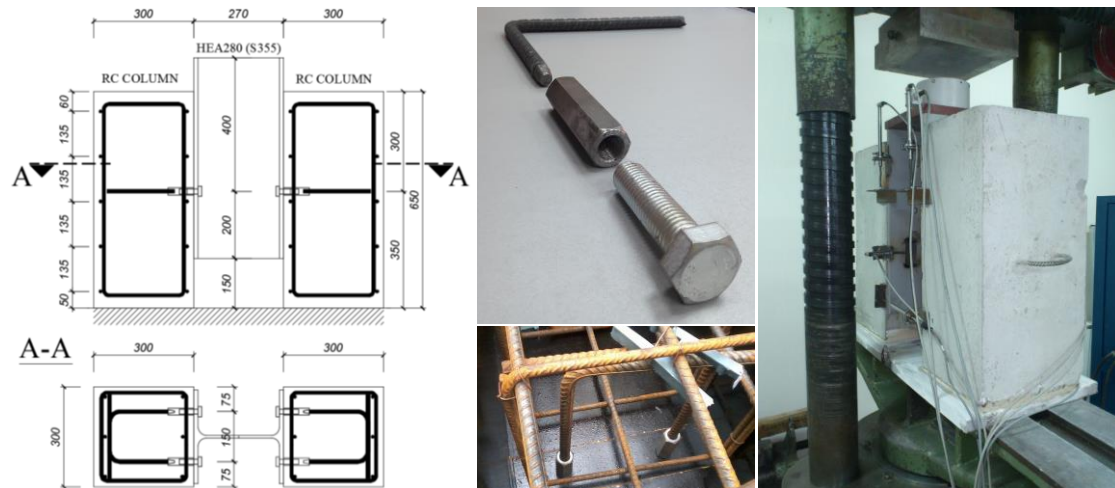


Fig. 1 Bolted connectors with mechanical and rebar anchor: geometry and preparation for testing of push-out specimens

Table 1 Component characteristics and relative resistance of test specimens (Milosavljević *et al.*, 2018)

| Series | Num. of spec. | Concrete edge distance c mm | Concrete strength f_{cm} MPa | Bolts | | Mechanical couplers | | Rebar anchor | Failure mode* | $P_{ult,mean}/F_{v,Rk}$ |
|--------|---------------|-------------------------------------|--------------------------------------|-------------|------------------|---------------------|----------------|--------------|---------------|-------------------------|
| | | | | Diameter | Tensile strength | Diameter | Length | Diameter | | |
| | | | | d_b mm | f_{ub} MPa | d_{co} mm | l_{co} mm | d_a mm | | |
| A | 4 | 75 | 26.60 | 16 | 837.67 | 22 | 59 | 12 | CEF | 1.160 |
| B | 4 | 75 | 26.86 | 16 | 837.67 | 22 | 59 | 12 | CEF | 1.207 |
| C | 4 | 100 | 37.72 | 16 | 837.67 | 22 | 59 | 12 | BSF | 1.215 |
| D | 3 | 150 | 32.58 | 16 | 907.00 | 22 | 79 | 12 | BSF | 1.044 |
| E | 3 | 150 | 39.41 | 20 | 948.00 | 27 | 93 | 16 | BSF | 0.996 |

*CEF = concrete edge failure, BSF = bolt shear failure

connectors. The general intention was to use these connectors for different types of shear connections in building and bridge construction, such as steel beam-concrete column connections and prefabricated composite beams. Therefore, the appropriate set of variables in this research was chosen to achieve two possible failure modes: concrete edge failure mode (characteristic for narrow members, e.g., haunches of concrete slabs in composite floors or RC columns) and bolt shear failure mode (characteristic for wide members, e.g., RC walls or concrete composite decks). It should be noted that the possibility of other failure modes, namely pullout and pryout failure modes, is excluded by sufficient anchorage length provided by long rebar anchor (see Fig. 1).

Push-out tests were performed on 18 specimens (5 series) according to Eurocode 4 (2004), with modified dimensions of concrete parts. As an example, the geometry of test specimens in series A is shown in Fig. 1. Testing of material characteristics of all parts of specimens was carried out using standard tests. The overview of the main geometrical and mechanical characteristics of the components of tested specimens in all series is given in Table 1.

Detail description of experimental research of bolted shear connectors with mechanical coupler and rebar anchor in different failure modes are given Milosavljević *et al.* (2018). In general, test specimens were arranged in two major groups with similar set of parameters and, consequently, similar behaviour under static shear load:

- The first group consisted of two specimen series (A and B), with small concrete edge distance and relatively low concrete compressive strength. Bolts M16 with compatible dimensions of mechanical coupler and rebar anchor were used (see Table 1). Specimens from series A and B differ in the amount of transverse reinforcement, with aim to investigate the influence of the degree of confinement on shear resistance. The specimens sustained concrete edge breakout failure (CEF), before reaching maximum measured force which corresponds to the bolt shear resistance.
- The second group consisted of three specimen series (C, D and E), with larger concrete edge distance and higher concrete compressive strength. The concrete edge distance and bolt diameter were varied. The specimens failed due to bolt shear failure (BSF) in one or two connectors.

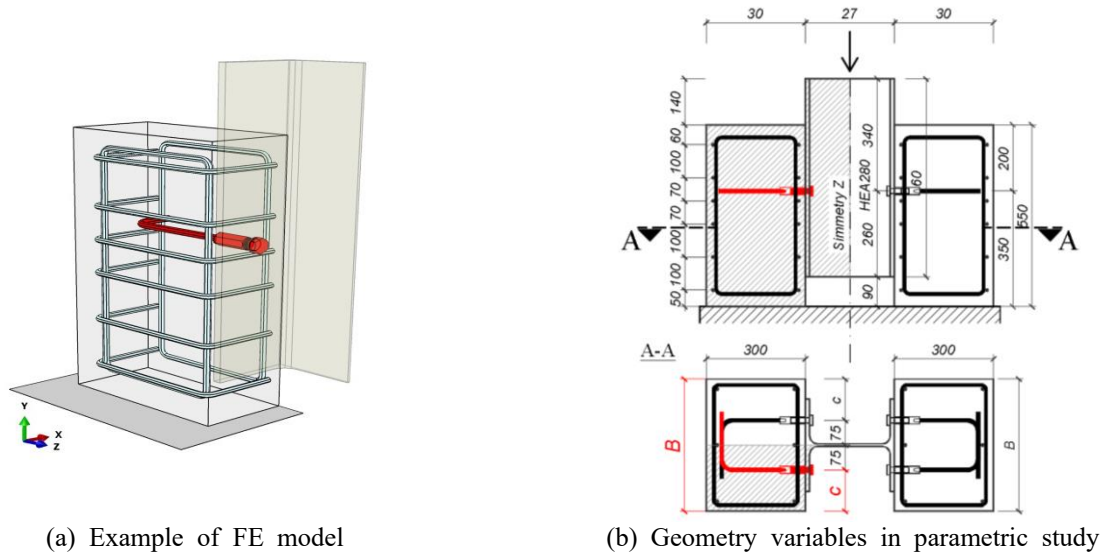


Fig. 2 Geometry of FE models used for parametric study

The ratios of the mean shear resistance obtained experimentally to shear resistance calculated according to EN 1993-1-8 are presented in Table 1. Shear resistances $F_{v,Rk}$ are adjusted to mean measured values of bolts strength f_{ub} for each specimen series, while section areas of threaded part of the bolts and $\alpha_v = 0.6$ are used. Higher ultimate capacity for specimens A and B, as opposed to pure shear resistance of bolts, was mainly attributed to the catenary effects, associated with higher displacements in concrete failure mode, and friction effects. The concrete breakout load of tested specimens was registered at around 70% of the ultimate resistance. Concrete breakout body was limited to the concrete cover in all cases, regardless of different degree of confinement (by stirrups) of specimens in series A and B. Therefore, it was concluded that the degree of confinement did not affect shear resistance of the connection. Shear resistance of most specimens which failed in bolt shear failure mode was similar to pure shear resistance of bolts, as shown in Table 1. Higher test-to-code resistance ratio for specimen series C as opposed to series D and E was attributed to the uncertainties related to friction effects in contact surfaces between steel member and concrete column.

3. FE parametric study

The experimental and numerical analyses conducted in Milosavljević *et al.* (2018) identified the concrete compressive strength, concrete edge distance and strength and diameter of bolts (i.e., mechanical coupler) as key parameters that govern failure mode and thus shear resistance and ductility capacity of bolted shear connections with mechanical coupler and rebar anchor. These parameters were considered in numerical parametric study, which is based on FE models built in Abaqus software that have been validated by push-out tests in Milosavljević *et al.* (2018), in terms of load-slip curves and exhibited type of

failure mode, at the global level, and concrete crushing and cracking, at the local level. The main objectives of the parametric study are: (1) to confirm the conclusions drawn in Milosavljević *et al.* (2018) regarding the overall behaviour and failure mode of this type of shear connectors on the larger range of key variables and (2) to obtain sufficient data as the basis for the development of calculation method for their shear resistance.

3.1 FE models

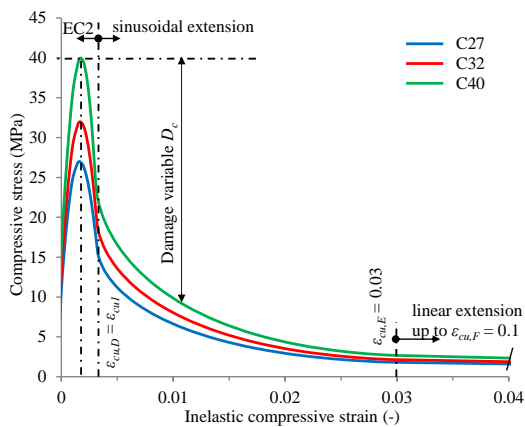
The geometry of numerical models used for the parametric study is given in Fig. 2. Owing to two axes of symmetry, only one quarter of specimen was modelled. All FE models correspond to the ones analysed in Milosavljević *et al.* (2018), regarding type and size of finite elements used for different parts of the connection, definition of contact interaction, boundary conditions and loading.

As shown in Table 2, the values of concrete edge distance c (i.e., width of concrete column B , Fig. 2), concrete compressive strength (concrete class) and bolt diameter were varied. Corresponding values are selected according to experimental tests in Milosavljević *et al.* (2018): (1) bolts M16 and M20, with corresponding dimensions of mechanical coupler and rebar anchor, (2) mean concrete compressive strength on standard cylinder $f_{cm} = 27\text{--}40$ MPa and (3) concrete edge distance $c = 75\text{--}150$ mm. For analysis purposes, the FE models were designated in the following order: M [bolt diameter] _C [concrete class] _ D [concrete edge distance]. A total number of 24 FE models were built and analysed.

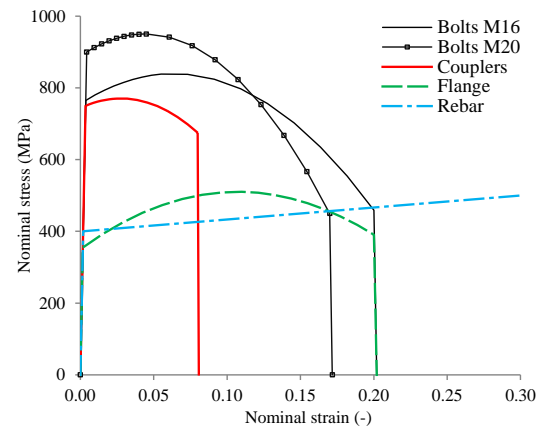
The mechanical behaviour of concrete and steel materials was defined using the uni-axial stress–strain relationship based on corresponding characteristics of tested material, as shown in Fig. 3. Concrete damage plasticity (CDP) model was used to model the behavior of concrete in compression and tension, defined by separate parameters. The compressive stress-strain curve (see Fig. 3(a)) was

Table 2 Values of key parameters considered in parametric study

| FE Model | M16 bolts (Rebar anchor Ø12) | | | | | M20 bolts (Rebar anchor Ø16) | | | | | |
|--------------|------------------------------|-----|-------------|----------------|-----------------|------------------------------|-----|-------------|----------------|-----------------|----|
| | B | c | Conc. class | Coupler | | B | c | Conc. class | Coupler | | |
| | | | | Diam. d_{co} | Length l_{co} | | | | Diam. d_{co} | Length l_{co} | |
| mm | mm | mm | mm | mm | mm | mm | mm | mm | mm | | |
| M16_C27_D75 | 300 | 75 | C27 | 22 | 59 | M20_C27_D75 | 300 | 75 | C27 | 27 | 93 |
| M16_C27_D100 | 350 | 100 | C27 | 22 | 59 | M20_C27_D100 | 350 | 100 | C27 | 27 | 93 |
| M16_C27_D125 | 400 | 125 | C27 | 22 | 59 | M20_C27_D125 | 400 | 125 | C27 | 27 | 93 |
| M16_C27_D150 | 450 | 150 | C27 | 22 | 59 | M20_C27_D150 | 450 | 150 | C27 | 27 | 93 |
| M16_C32_D75 | 300 | 75 | C32 | 22 | 59 | M20_C32_D75 | 300 | 75 | C32 | 27 | 93 |
| M16_C32_D100 | 350 | 100 | C32 | 22 | 59 | M20_C32_D100 | 350 | 100 | C32 | 27 | 93 |
| M16_C32_D125 | 400 | 125 | C32 | 22 | 59 | M20_C32_D125 | 400 | 125 | C32 | 27 | 93 |
| M16_C32_D150 | 450 | 150 | C32 | 22 | 59 | M20_C32_D150 | 450 | 150 | C32 | 27 | 93 |
| M16_C40_D75 | 300 | 75 | C40 | 22 | 59 | M20_C40_D75 | 300 | 75 | C40 | 27 | 93 |
| M16_C40_D100 | 350 | 100 | C40 | 22 | 59 | M20_C40_D100 | 350 | 100 | C40 | 27 | 93 |
| M16_C40_D125 | 400 | 125 | C40 | 22 | 59 | M20_C40_D125 | 400 | 125 | C40 | 27 | 93 |
| M16_C40_D150 | 450 | 150 | C40 | 22 | 59 | M20_C40_D150 | 450 | 150 | C40 | 27 | 93 |



(a) Concrete material model in compression



(b) Material models for steel components

Fig. 3 Material models for parametric study

defined according to Eurocode 2 (2004) up to strain $\varepsilon_{cu1} = 3.5 \cdot 10^{-3}$, followed by the combination of sinusoidal extension for strains in range $\varepsilon_c = 3.5 \cdot 10^{-3} - 30 \cdot 10^{-3}$ and linear extension up to $\varepsilon_{cu,F} = 100 \cdot 10^{-3}$, as described in (Pavlović *et al.* 2013, Milosavljević *et al.* 2018). Mechanical properties of concrete used in parametric study are calculated according to Eurocode 2 (2004) and given in Table 3. Detail description of all parameters used to model the behaviour of concrete is given in Milosavljević *et al.* (2018). The stress–strain relationship of different steel materials is given in Fig. 3(b). Ductile damage model was defined for bolts, coupler and steel section. In addition, shear damage model was used for bolts, as described by Milosavljević *et al.* (2018) and Milosavljević (2014). The most important mechanical properties of steel parts are given in Table 4.

Table 3 Mechanical characteristics of concrete used in parametric study

| Concrete class | f_{cm} | f_{ctm} | E_{cm} |
|----------------|----------|-----------|----------|
| | MPa | MPa | MPa |
| C27 | 27.0 | 2.14 | 29637.0 |
| C32 | 32.0 | 2.5 | 31187.0 |
| C40 | 40.0 | 3.0 | 33346.0 |

Table 4 Mechanical characteristics of steel parts used in parametric study

| Part of connector assembly | f_{02} | f_{ub} | ε_u | E_s |
|----------------------------|----------|----------|-----------------|-------|
| | MPa | MPa | % | GPa |
| Bolts M16 | 765.0 | 838.0 | 20.0 | 210.0 |
| Bolts M20 | 900.0 | 950.0 | 17.0 | 210.0 |
| Coupler | 750.0 | 770.0 | 8.0 | 195.0 |
| Rebar anchor | 400.0 | 500.0 | 20.0 | 210.0 |

Table 5 Results of the parametric study

| FE model | M16 bolts ($d_{co} = 22$ mm, $l_{co} = 59$ mm, $d_a = 12$ mm) | | | FE model | M20 bolts ($d_{co} = 27$ mm, $l_{co} = 93$ mm, $d_a = 16$ mm) | | |
|--------------|---|------------------------|---------------|--------------|---|------------------------|---------------|
| | $P_{ult,FEM}$ kN | $\delta_{u,FEM}$ mm | Failure mode* | | $P_{ult,FEM}$ kN | $\delta_{u,FEM}$ mm | Failure mode* |
| M16_C27_D75 | 102.3 | 5.41 | CEF | M20_C27_D75 | 172.6 | 8.09 | CEF |
| M16_C27_D100 | 101.6 | 4.65 | CEF | M20_C27_D100 | 165.1 | 5.84 | CEF |
| M16_C27_D125 | 99.9 | 3.97 | CEF/BSF | M20_C27_D125 | 159.6 | 4.67 | CEF |
| M16_C27_D150 | 96.1 | 3.58 | BSF | M20_C27_D150 | 155.4 | 3.91 | CEF |
| M16_C32_D75 | 100.7 | 4.66 | CEF | M20_C32_D75 | 166.3 | 5.99 | CEF |
| M16_C32_D100 | 99.1 | 3.61 | CEF | M20_C32_D100 | 160.1 | 4.65 | CEF |
| M16_C32_D125 | 94.6 | 2.90 | BSF | M20_C32_D125 | 154.4 | 3.71 | CEF |
| M16_C32_D150 | 94.8 | 2.54 | BSF | M20_C32_D150 | 151.8 | 3.41 | CEF/BSF |
| M16_C40_D75 | 99.6 | 3.91 | CEF | M20_C40_D75 | 162.2 | 4.94 | CEF |
| M16_C40_D100 | 95.6 | 2.87 | CEF/BSF | M20_C40_D100 | 154.1 | 3.62 | CEF |
| M16_C40_D125 | 93.4 | 2.28 | BSF | M20_C40_D125 | 151.2 | 3.34 | CEF/BSF |
| M16_C40_D150 | 93.9 | 2.25 | BSF | M20_C40_D150 | 152.9 | 3.11 | BSF |

*CEF = concrete edge failure, BSF = bolt shear failure, CEF/BSF = combined failure

3.2 FE results

The ultimate connection resistance $P_{ult,FEM}$ and ultimate vertical slip $\delta_{u,FEM}$ of FE models from parametric study are given in Table 5. Ultimate vertical slip was determined as a value of slip obtained from the end of cycling loading to the point at 90% of the ultimate connection resistance, on descending part of the load-slip curve. Load-slip curves per connector for different bolt diameters, concrete strengths and concrete edge distances are presented in Fig. 4. Only load-slip curves for concrete classes C27 (lowest considered) and C40 (highest considered) are shown, to represent boundaries of global behaviour of shear connectors with mechanical coupler within the range of variables considered in parametric study presented in this paper. Although ultimate resistance of connections corresponds to the bolt shear resistance in all cases, FE models exhibited different failure modes which reflected on their global behaviour, as shown in Fig. 4.

3.2.1 Failure modes

Fig. 5 shows two possible failure modes for bolted shear connectors with mechanical coupler analysed in FE parametric study, which are described by deformed shapes and plots of the variable of tension damage in concrete (DAMAGET) at the ultimate shear resistance of the connections. As an example, the comparison of damage patterns and failure modes of cases with different concrete edge distances and bolt diameters but with the same concrete class (class C40, see Table 3) is shown. Regardless of bolt diameter, connections with small concrete edge distance, $c = 75$ mm, exhibit concrete edge breakout failure before reaching ultimate connection resistance while connections with large edge distance, $c = 150$ mm, exhibit bolt shear failure without significant cracking in concrete.

In case of concrete edge breakout failure ($c = 75$ mm), inclined tensile cracks, presented as DAMAGET variable on Fig. 5, propagated fully from the connector to the concrete edge, and thus formed typical concrete edge breakout body, similar to those observed in experimental tests conducted in Milosavljević *et al.* (2018) and Grosser (2012). Concrete damage is more severe in case of larger diameter (and lower concrete class), resulting in higher connection slip, as shown in Fig. 4. Although similar conclusion applies for FE models with $c = 150$ mm which failed in bolt shear failure mode, concrete damage is quite limited, with one or no inclined tensile cracks, as shown in Fig. 5.

For the purpose of further analysis and development of calculation model for shear resistance of bolted connectors with mechanical coupler, an attempt to designate failure modes of all FE models as either bolt shear failure (BSF) or concrete edge failure mode (CEF) was made. The point of total propagation of inclined cracks (DAMAGET variable) towards the concrete edge, observed on the section A-A shown in Fig. 5, was set as the condition for classification of failure mode as concrete edge failure mode. The corresponding shear load is designated as concrete edge breakout resistance $V_{u,c}$, used for derivation of calculation model in Section 4. It should be noted, however, that the concrete edge breakout load does not represent the ultimate resistance of the connection because concrete breakout body is limited to the concrete cover only, which was observed experimentally and verified numerically by Milosavljević *et al.* (2018). FE models designated as CEF in Table 5 met the adopted condition whereas FE models designated as BSF did not meet the same condition.

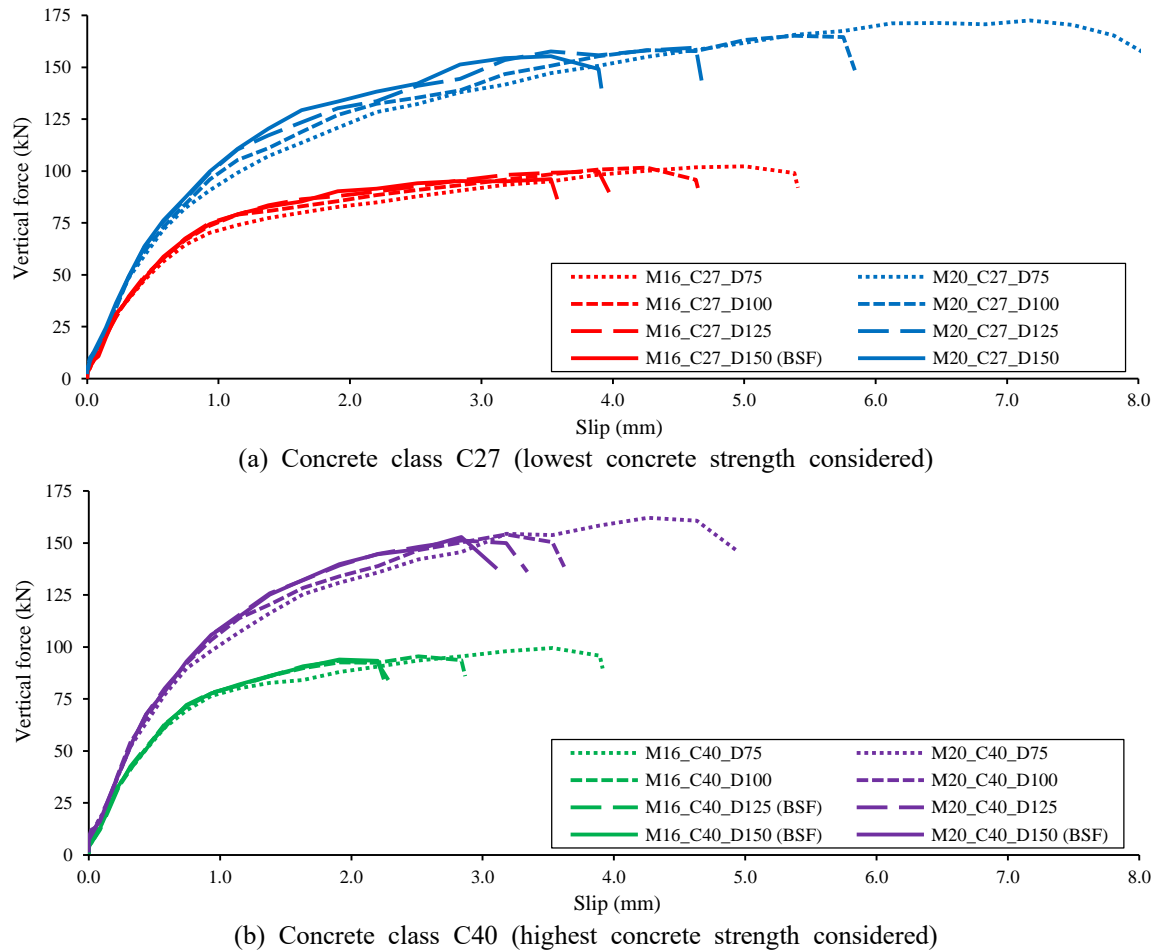


Fig. 4 Force-slip curves from the parametric study

In cases when total propagation of inclined cracks towards concrete edge coincided with bolt shear failure (without clear distinction between failure modes), the failure mode of FE model was designated as combined failure mode (CEF/BSF in Table 5). The degree of damage and distribution of cracks in concrete part of the connection (DAMAGET variable) as well as shear stresses and deformation of M16 bolts (S23 variable) at the ultimate shear resistance, for different concrete strengths (C27 and C40) and edge distances ($c = 75-150$ mm), are presented in Fig. 6. It can be noticed from Fig. 6 (and Table 5) that, in most cases, the variation of concrete edge distance and/or concrete strength leads to different failure modes of FE models with the same bolt diameter.

Although all FE models ultimately failed in shear failure of bolts, the contribution of shear stress to the failure criterion is dependent on the concrete strength and edge distance due to amount of rotation of connector's axis, see Fig. 6. Higher values and concentration of shear stresses (S23 stresses) are noticed in Fig. 6 in case of bolt shear failure modes as a result of lower rotation of connector's axis – for the same concrete strength the rotation is more than two times lower in case BSF compared to CEF mode. The detailed analysis of the values of shear force/axial force/bending moment in bolted connector with mechanical

coupler and rebar anchor for different failure modes is given in Milosavljević *et al.* (2018).

3.2.2 Shear connection stiffness, resistance and ductility

The results of parametric study have shown that all FE models have similar behaviour in the elastic range, which is consistent with test results described in Milosavljević *et al.* (2018). High initial stiffness is the result of large bearing surface of mechanical coupler, and it is higher in case of connectors with M20 bolts compared to the stiffness of the connectors with M16 bolts. The relatively early onset of nonlinearity comes from the thread penetration into the hole surface which is typical for bolted and demountable connections, such as those used in Pavlović and Veljković (2017), Pathirana *et al.* (2016) and Dai *et al.* (2015).

The variation of the connector stiffness k_{sc} , defined in Eurocode 4 (2004) by the ratio of $0.7P_{ult}$ to the corresponding slip from force-slip curves, for different bolt diameters, concrete edge distances and concrete strengths is shown in Fig. 7. Shear stiffness k_{sc} per connector is in range of 71-103 kN/mm in case of M16 bolts and in range of 63-114 kN/mm in case of M20 bolts. It is evident that shear stiffness k_{sc} is affected by all three parameters considered and, consequently, it strongly depends on the type of failure

Concrete edge failure (CEF)

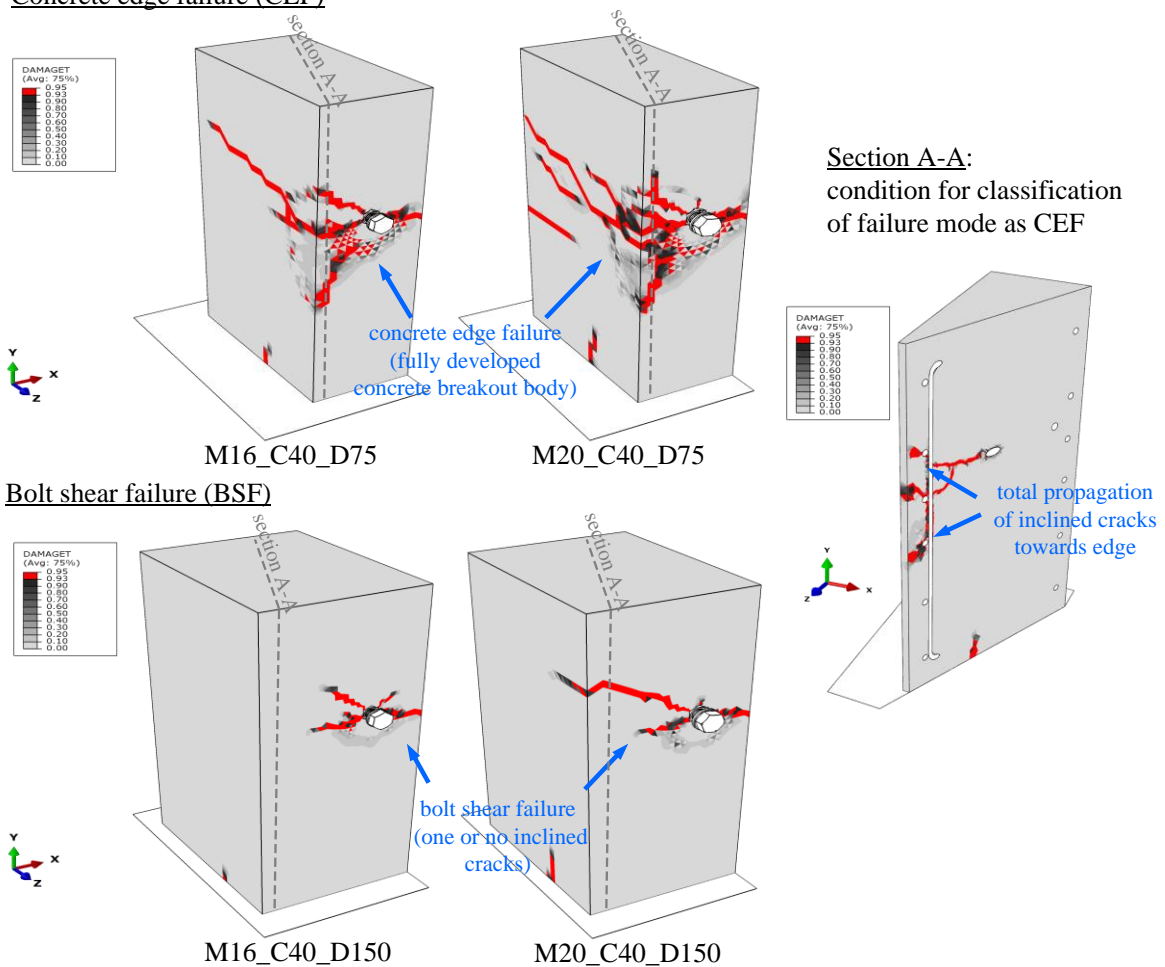


Fig. 5 Failure modes and damage patterns of FE models

mode of the connector. Shear stiffness is markedly low in case of concrete failure mode since concrete edge breakout failure is generally attained at load levels around $0.7P_{ult}$ (see $V_{u,c}/P_{ult}$ ratios in Tables 8 and 9); because of the lower $V_{u,c}/P_{ult}$ ratio for M20 bolts compared to M16 bolts, the reduction of stiffness is more pronounced. In case of bolt shear failure, shear stiffness is almost unaffected by concrete edge distance (Fig. 7(a)) and it is higher when higher concrete classes and larger bolt diameters are used. In this failure mode, shear stiffness of the connector with mechanical coupler ($k_{sc} = 103.3$ kN/mm for M16 bolts and concrete class C40), is higher when compared to bolted connectors with single embedded nut ($k_{sc} = 68.0$ kN/mm, as reported by Pavlović *et al.* 2013) but lower when compared to welded headed studs ($k_{sc} = 122.0$ kN/mm, as reported by Spremić *et al.* 2013) with the same diameter and similar concrete class.

Fig. 8 shows the effect of changing bolt diameter, concrete edge distance and concrete strength on the ultimate shear resistance and vertical slip of bolted connectors with mechanical coupler. Similar to the case of shear stiffness, ultimate load and slip of the connection also strongly depend on which type of failure mode is attained.

The results have shown that the behaviour of connections, which failed in bolt shear failure mode, cannot be classified as ductile according to Eurocode 4 (2004) since the ultimate slip is, in all cases, lower than minimum required value of 6 mm. For the range of parameters considered, the ductility can somewhat be increased by using lower concrete class or larger bolt diameter, as shown in Fig. 8(b). Figs. 4 and 8(b) show that concrete edge breakout type of failure provides considerably higher ultimate ductility capacity of the connection when compared to the shear failure of bolts. Depending on the concrete class, reduction of concrete edge distance, from $c = 150$ mm to $c = 75$ mm, gives an increase of the ultimate slip by 51-83% for M16 bolts and by 59-107% for M20 bolts. It should be mentioned, however, that concrete breakout failure is attained at significantly lower slip of the connection, in range of 1-2 mm. In general, the increase of bolt diameter from M16 to M20 increases the connection slip, from 10% to 50% depending on the type of failure mode.

The obtained results have also shown that, for the same bolt diameter, shear resistance of the connection increases with decreasing concrete edge distance and concrete strength, as a result of changing the failure mode from bolt

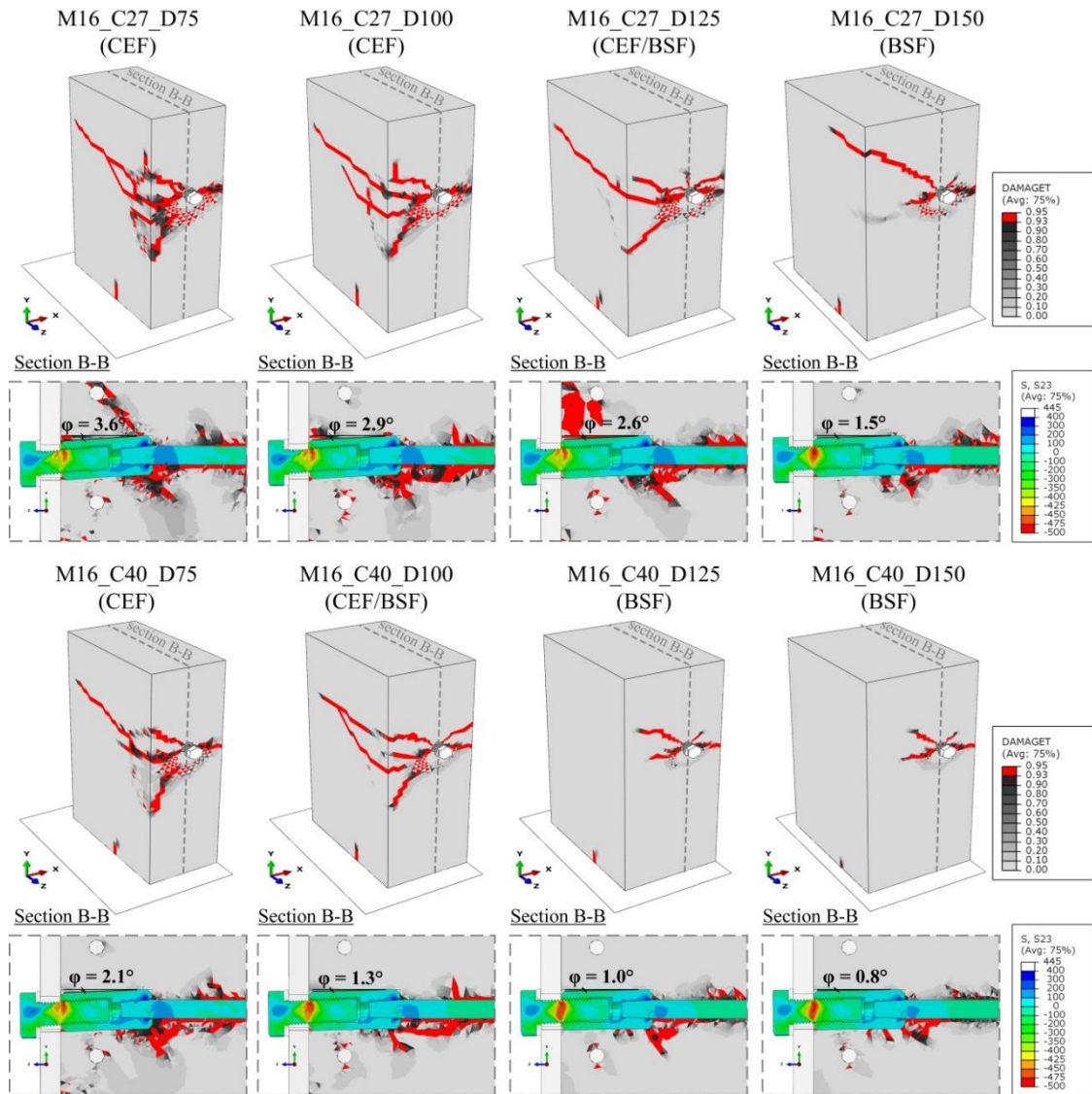


Fig. 6 FEM analysis: failure modes, damage patterns and shear stresses in M16 bolts for models with concrete compressive strength C27 and C40

shear failure to concrete edge failure (see Fig. 8(a)). The reduction of concrete edge distance solely, from $c = 150$ mm to $c = 75$ mm, increases shear resistance by approximately 6% and 10% for M16 bolts and M20 bolts, respectively. The increase of bearing capacity is related to the higher degree of concrete damage, larger vertical slip and corresponding rotation of connector's axis which, due to catenary effects, leads to more ductile failure mode of the bolt, loaded by the combination of shear, tension and bending. The comparison of the internal forces in shear connector with mechanical coupler for two failure modes is given and explained in Milosavljević *et al.* (2018).

4. Shear resistance of bolted connectors with mechanical coupler

The results of the parametric study described in Section 3 confirmed the conclusions drawn from experimental and

numerical studies presented in Milosavljević *et al.* (2018), regarding the influence of key parameters on the failure modes of connectors with mechanical coupler and rebar anchor. Both studies have identified two possible failure modes of these connectors loaded in shear: steel (bolt) failure and concrete edge failure. Therefore, the design equations for shear resistance in each failure mode are developed based on the results of corresponding experimental tests and numerical models. In addition, the limiting values of key parameters that govern failure modes are also discussed.

4.1 Resistance of shear connectors with mechanical coupler without the influence of concrete edge distance

If located far enough from the concrete edge, shear resistance of bolted connectors with mechanical coupler as well as the other types of bolted connectors with sufficient length (to prevent pryout and pullout failures) will be

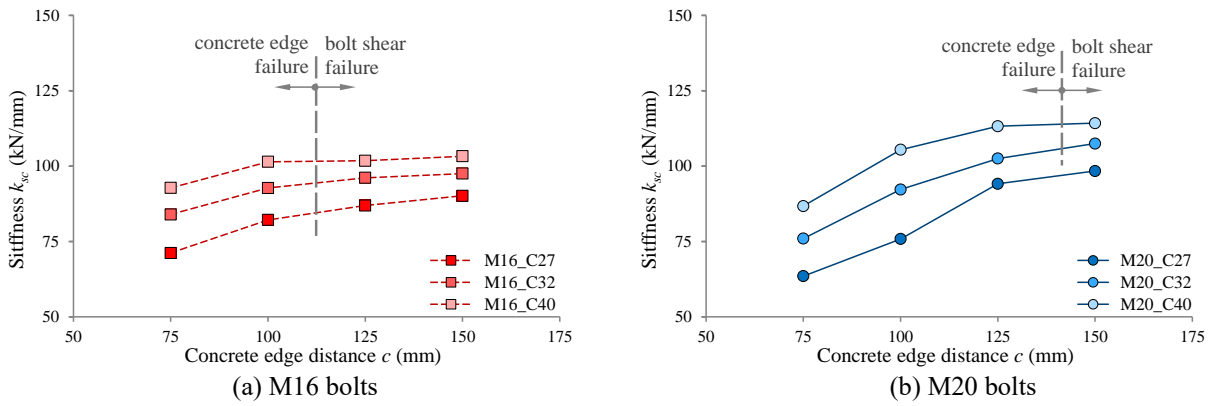
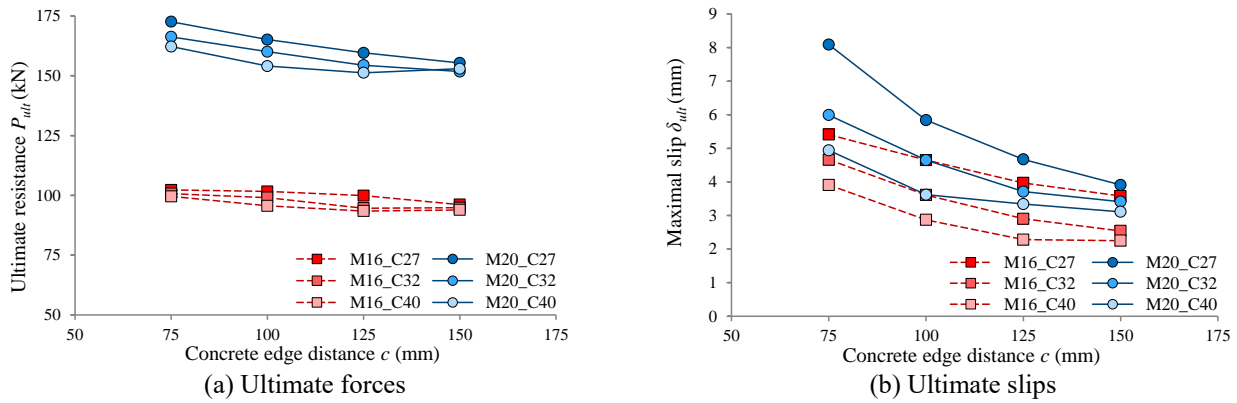
Fig. 7 Parametric study: stiffness k_{sc} per shear connector

Fig. 8 Parametric study: ultimate forces and vertical slips for different bolt diameters, concrete edge distances and concrete strengths

governed by shear capacity of bolts. Shear resistance in this failure mode is often defined as the product of the ultimate tensile resistance of bolts and shear resistance factor α_v , according to Eq. (1):

$$F_{v,Rk} = \alpha_v f_{ub} A_{net} \quad (1)$$

where f_{ub} and A_{net} are tensile strength and tensile stress area of the bolts, respectively.

There are several recommendations in the literature for the values of shear resistance factor α_v , in design of different types of shear connections. Eurocode 3 (2005) prescribes the values of $\alpha_v = 0.6$, for bolt classes 4.6, 5.6, 8.8, and $\alpha_v = 0.5$, for bolt classes 4.8, 5.8, 6.8, 10.9, when shear plane passes through the threaded portion of the bolt. CEB-FIP (2011) recommends the value of 0.5 for cast-in and post-installed anchors, regardless of anchor tensile strength. For the same type of anchors, Grosser (2012) proposed the value of $\alpha_v = 0.6$, for f_{ub} in range of 500-1000 MPa. The reduction factor, which depends of the rupture elongation of the anchor, is also defined. However, there is no reduction if the rupture elongation is greater than 16%. Based on experimental tests, Yang *et al.* (2018) measured the value of $\alpha_v = 0.8$ for shear connectors assembled from short bolt, mechanical coupler and long bolt (instead of rebar anchor, used in this paper). It was noted that the shear

resistance factor is much higher than the value of $1/\sqrt{3}$ according to Mises criterion and that further analyses were needed. According to Pavlović *et al.* (2013), friction and contact forces acting on embedded nut and concrete as well as the catenary effects in bolt increase the shear resistance of bolted connectors with single embedded nut as opposed to the pure shear resistance of bolts.

The summary of the ultimate connection resistances for bolt shear failure mode obtained from parametric study presented in Table 5 (designated as BSF) and corresponding FE models presented in Milosavljević *et al.* (2018) are given in Table 6. It can be noted that the values of shear resistance factor α_v for both M16 and M20 bolts are higher than the value of 0.6. Since ductile and shear damage models were calibrated to match real bolt material, pure shear resistance of bolts is approximately equal to $0.6f_{ub}A_s$, in all cases. The additional bearing capacity arises from friction and contact forces acting on mechanical coupler and concrete and catenary effects, similarly as in case of bolted shear connectors with single embedded nut. Based on the values of α_v presented in Table 6, it can be concluded that these effects depend neither on concrete strength nor on concrete edge distance. Hence, the main influencing factor is the bolt diameter. Furthermore, the effects are less pronounced for M20 bolts than for M16 bolts, owing to the

Table 6 Resistance of bolted connectors with mechanical coupler – bolt shear failure

| FE model | <i>Bolt diameter</i> | f_{cm} | c | $P_{ult,FEM}$ | A_{net} | f_{ub} | $A_{netf_{ub}}$ | $\alpha_v = P_{ult,FEM}/A_{netf_{ub}}$ | $\alpha_{v,mean}$ |
|--------------|----------------------|----------|-----|---------------|-----------------|----------|-----------------|--|-------------------|
| | mm | MPa | mm | kN | mm ² | MPa | kN | | |
| M16_C27_D150 | 16 | 27.0 | 150 | 96.1 | 157.0 | 838.0 | 131.6 | 0.730 | |
| M16_C32_D125 | 16 | 32.0 | 125 | 94.6 | 157.0 | 838.0 | 131.6 | 0.719 | |
| M16_C32_D150 | 16 | 32.0 | 150 | 94.8 | 157.0 | 838.0 | 131.6 | 0.721 | 0.72 |
| M16_C40_D125 | 16 | 40.0 | 125 | 93.4 | 157.0 | 838.0 | 131.6 | 0.710 | |
| M16_C40_D150 | 16 | 40.0 | 150 | 93.9 | 157.0 | 838.0 | 131.6 | 0.714 | |
| FEM_C* | 16 | 38.0 | 100 | 96.5 | 157.0 | 838.0 | 131.6 | 0.733 | |
| M20_C40_D150 | 20 | 40.0 | 150 | 152.9 | 245.0 | 950.0 | 232.8 | 0.657 | 0.65 |
| FEM_E* | 20 | 40.0 | 150 | 148.1 | 245.0 | 950.0 | 232.8 | 0.636 | |

*from Milosavljević *et al.* (2018)

higher bearing stiffness of M20 bolts and corresponding mechanical coupler. According to Table 6, mean values of shear resistance factor, obtained from numerical analysis, are $\alpha_v = 0.72$ for M16 bolts and $\alpha_v = 0.65$ for M20 bolts. Pavlović (2014) numerically obtained similar values of shear resistance factor for bolted connectors with single embedded nut and showed that α_v factor decreases with further increase of bolt diameter, up to $\alpha_v = 0.6$ for M34 bolts.

4.2 Resistance of shear connectors with mechanical coupler located close to the concrete edge

When located close to the edge of concrete members, shear connections are potentially exposed to severe concrete damage in the vicinity of the edge. Previously conducted experiments and FE analyses of bolted connections with mechanical coupler, which failed by breakout of concrete edge, have shown that concrete damage is limited to the concrete cover around the edge while the concrete core within the stirrups remains undamaged. The remaining concrete provides sufficient bearing surface to enable further increase of shear load on the connection, resulting in even higher ultimate resistance and slip when compared to bolt shear failure mode (up to 10% and 107%, respectively). Still, determining the concrete edge breakout capacity in order to predict overall behaviour of the connection remains of primary importance and, to the authors' opinion, should be considered as limit state in the design of connection.

The proposed model for concrete edge breakout resistance of bolted shear connectors with mechanical coupler and rebar anchor is based on the analogy of its behaviour with the behaviour of cast in and post-installed anchors loaded parallel to the concrete edge. The conclusion of similar behaviour of these two types of anchors was drawn by comparison of concrete damages and characteristic crack patterns associated with concrete edge breakout failure, shown on FE models in Fig. 5 and on tested specimens in Milosavljević *et al.* (2018) and Grosser (2012). Furthermore, Grosser (2012) highlighted concrete edge distance, concrete strength and anchor diameter and

length as key parameters that affect shear resistance of anchors loaded parallel to the concrete edge. Similarly, the results of experimental and numerical study presented in Milosavljević *et al.* (2018) indicated that the combination of small edge distance, low concrete strength and/or high shear strength of bolts can lead to the concrete edge breakout failure of bolted shear connections with mechanical couplers. These observations were confirmed by the results of the FE parametric study presented in Section 3.

Grosser (2012) has developed a relatively simple model for hand calculation of concrete edge failure load of shear anchors loaded parallel to the concrete edge. The model was based on 118 test results and numerical analysis on corresponding FE models. Experimental database comprised test results of specimens with following characteristics: (1) concrete edge distance in range of 45-200 mm, (2) concrete compressive strength in range of 23-36 MPa (low strength concrete) and 61-84 MPa (high strength concrete), (3) threaded rod diameter in range of 12-24 mm, and (4) embedment depth in range of 80-320 mm. The numerical analysis extended the range of concrete compressive strength by considering the values between 25 MPa and 70 MPa, as well as the range of anchor diameter by considering anchors with diameters between 10 and 60 mm. The obtained model showed very good match with experimental test results. The mean value of shear resistance $V_{u,c}$ is given according to Eq. (2).

$$V_{u,c} = 43 \cdot \sqrt{f_{cc,200}} \cdot c^{2/3} \cdot d \cdot \psi_{l,v} \quad (2)$$

where

- $f_{cc,200}$ mean concrete compressive strength measured on cubes with a side length of 200 mm (in MPa); according to EN 206-1, $f_{cc,200} = f_{cm}/0.84$, where f_{cm} is concrete compressive strength measured on 150/300 mm cylinders
- c concrete edge distance (in mm)
- d anchor diameter (in mm)
- $\psi_{l,v}$ reduction factor expressing the influence of the anchor stiffness on concrete edge failure load

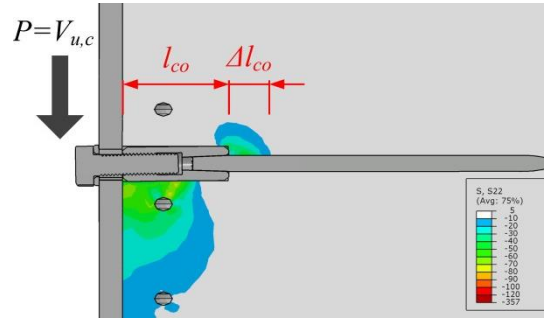


Fig. 9 Definition of activated length of rebar anchor

Table 7 Activated length Δl_{co} of rebar anchor and stiffness ratio $l_{f,eq}/d_{co}$

| M16 bolts ($d_a = 12$ mm, $d_{co} = 22$ mm, $l_{co} = 59$ mm) | | | | | M20 bolts ($d_a = 16$ mm, $d_{co} = 27$ mm, $l_{co} = 93$ mm) | | | | |
|---|-----------------|---------------------------|--|-------------------|---|-----------------|---------------------------|--|-------------------|
| FE model | f_{cm} MPa | $\Delta l_{co,FEM}$ mm | $\Delta l_{co,FEM}/$ $\Delta l_{co,Eq.(6)}$ | $l_{f,eq}/d_{co}$ | FE model | f_{cm} MPa | $\Delta l_{co,FEM}$ mm | $\Delta l_{co,FEM}/$ $\Delta l_{co,Eq.(6)}$ | $l_{f,eq}/d_{co}$ |
| FEM_A* | 27.0 | 32.0 | 1.08 | 3.42 | M20_C27_D75 | 27.0 | 36.0 | 1.05 | 4.20 |
| M16_C27_D75 | 27.0 | 31.0 | 1.04 | 3.42 | M20_C27_D100 | 27.0 | 34.5 | 1.01 | 4.20 |
| M16_C27_D100 | 27.0 | 28.0 | 0.94 | 3.42 | M20_C27_D125 | 27.0 | 34.0 | 0.99 | 4.20 |
| M16_C27_D125 | 27.0 | 28.0 | 0.94 | 3.42 | M20_C27_D150 | 27.0 | 32.0 | 0.93 | 4.20 |
| M16_C32_D75 | 32.0 | 27.0 | 0.97 | 3.37 | M20_C32_D75 | 32.0 | 32.0 | 0.99 | 4.15 |
| M16_C32_D100 | 32.0 | 27.0 | 0.97 | 3.37 | M20_C32_D100 | 32.0 | 30.0 | 0.93 | 4.15 |
| M16_C40_D75 | 40.0 | 25.0 | 0.98 | 3.32 | M20_C32_D125 | 32.0 | 29.0 | 0.90 | 4.15 |
| M16_C40_D100 | 40.0 | 27.0 | 1.06 | 3.32 | M20_C32_D150 | 32.0 | 31.0 | 0.96 | 4.15 |
| | | | | | M20_C40_D75 | 40.0 | 30.0 | 1.02 | 4.09 |
| | | | | | M20_C40_D100 | 40.0 | 30.0 | 1.02 | 4.09 |
| | | | | | M20_C40_D125 | 40.0 | 31.0 | 1.05 | 4.09 |

*from Milosavljević *et al.* (2018)

Coefficient $\psi_{l,V}$ is given according to Eq. (3). It is defined as a function of anchor stiffness l_f/d , where l_f is the influence length of the anchor loaded in shear. For anchors with constant diameter over the embedment depth, l_f equals to the embedment depth of the anchor.

$$\psi_{l,V} = \left(\frac{l_f}{12d} \right)^x \quad \text{with: } x = \begin{cases} 0.3 & \text{for } \frac{l_f}{d} < 12 \\ 0 & \text{for } \frac{l_f}{d} > 12 \end{cases} \quad (3)$$

The experimental and numerical results in Grosser (2012) showed that the increase of stiffness ratio l_f/d above the value of 12 is ineffective, since it does not lead to an increase of the concrete edge breakout load. Hence, the limiting value of stiffness ratio l_f/d is set to 12. Although CEB-FIP (2011) recommends different calculation models, the limiting values of stiffness ratio are quite similar: $l_f/d \leq 12$ for anchor diameter $d_{nom} \leq 24$ mm, and $l_f/d < 8$ for anchor diameter $d_{nom} > 24$ mm.

4.2.1 The influence length of shear connectors with mechanical coupler

According to Grosser (2012), calculation model for

concrete edge breakout load, given by Eq. (2), is derived for anchors with constant diameter over the embedment depth. Consequently, its application for shear connectors with mechanical coupler is not straightforward, since there is no guidance for determination of the influence length l_f for anchors with variable diameter. Substituting the value of large embedment depth, provided by the long rebar anchor, in combination with either diameter of mechanical coupler or diameter of rebar anchor in Eq. (2) would yield incorrect results because of large difference between coupler and anchor diameters (see Table 2). To the authors' knowledge, there are no recommendations for these types of anchors in any design guides, reports or codes beyond the requirement to determine the influence length for particular anchor from test results. In this paper, the results of FE study are used to determine the appropriate influence length of shear connectors with mechanical coupler in order to implement Eq. (2) in their design.

Distribution of vertical stresses in concrete around the shear connector with mechanical coupler at the stage of concrete edge failure attainment, defined in Section 3.2.1, is presented on Fig. 9. It can be noticed that the shear load is transferred from the connector to the surrounding concrete through the bearing area of mechanical coupler and one

Table 8 Concrete edge breakout load of test specimens from Milosavljević *et al.* (2018)

| Test specimen (M16 bolts) | f_{cm} | c | $V_{u,c, test}^*$ | $V_{u,c, test}/P_{ult}$ | $V_{u,c, test, mean}$ | s_x | V_x (%) | $\delta_{u,c}$ | $\delta_{u,c, mean}$ | s_x | V_x (%) |
|------------------------------|----------|-----|-------------------|-------------------------|-----------------------|-------|-----------|----------------|----------------------|-------|-----------|
| | MPa | mm | kN | | | | | mm | mm | | |
| A1 | | | 64.3 | 0.740 | | | | 1.27 | | | |
| A2 | 26.6 | 75 | 60.5 | 0.770 | 67.50 | 3.13 | 6.59 | 1.22 | 1.21 | 0.07 | 6.17 |
| A3 | | | 70.5 | 0.737 | | | | 1.10 | | | |
| A4 | | | 67.8 | 0.737 | | | | 1.24 | | | |
| B1 | | | 62.3 | 0.710 | | | | 1.01 | | | |
| B2 | 26.9 | 75 | 74.0 | 0.712 | 65.69 | 5.58 | 8.49 | 1.28 | 1.11 | 0.12 | 10.92 |
| B3 | | | 63.8 | 0.675 | | | | 1.04 | | | |
| B4 | | | 62.8 | 0.661 | | | | 1.10 | | | |

*per one shear connector

Table 9 Summary of concrete edge breakout load for FE models

| FE model | M16 bolts ($d_a = 12$ mm, $d_{co} = 22$ mm, $l_{co} = 59$ mm) | | | | | FE model | M20 bolts ($d_a = 16$ mm, $d_{co} = 27$ mm, $l_{co} = 93$ mm) | | | | |
|--------------|---|-----|-------------|----------------|-----------------------------|--------------|---|-----|-------------|----------------|-----------------------------|
| | f_{cm} | c | $l_{f, eq}$ | $V_{u,c, FEM}$ | $V_{u,c, FEM}/P_{ult, FEM}$ | | f_{cm} | c | $l_{f, eq}$ | $V_{u,c, FEM}$ | $V_{u,c, FEM}/P_{ult, FEM}$ |
| | MPa | mm | mm | kN | | | MPa | mm | mm | kN | |
| FEM_A* | 27.0 | 75 | 75.2 | 68.6 | 0.697 | M20_C27_D75 | 27.0 | 75 | 113.3 | 90.8 | 0.526 |
| M16_C27_D75 | 27.0 | 75 | 75.2 | 64.4 | 0.630 | M20_C27_D100 | 27.0 | 100 | 113.3 | 105.4 | 0.638 |
| M16_C27_D100 | 27.0 | 100 | 75.2 | 79.0 | 0.778 | M20_C27_D125 | 27.0 | 125 | 113.3 | 123.5 | 0.774 |
| M16_C27_D125 | 27.0 | 125 | 75.2 | 92.8 | 0.929 | M20_C27_D150 | 27.0 | 150 | 113.3 | 138.3 | 0.890 |
| M16_C32_D75 | 32.0 | 75 | 74.2 | 74.0 | 0.735 | M20_C32_D75 | 32.0 | 75 | 112.1 | 94.4 | 0.567 |
| M16_C32_D100 | 32.0 | 100 | 74.2 | 86.3 | 0.871 | M20_C32_D100 | 32.0 | 100 | 112.1 | 110.6 | 0.691 |
| M16_C40_D75 | 40.0 | 75 | 73.0 | 76.4 | 0.768 | M20_C32_D125 | 32.0 | 125 | 112.1 | 129.0 | 0.835 |
| M16_C40_D100 | 40.0 | 100 | 73.0 | 92.5 | 0.968 | M20_C32_D150 | 32.0 | 150 | 112.1 | 147.6 | 0.972 |
| | | | | | | M20_C40_D75 | 40.0 | 75 | 110.5 | 98.2 | 0.605 |
| | | | | | | M20_C40_D100 | 40.0 | 100 | 110.5 | 120.4 | 0.782 |
| | | | | | | M20_C40_D125 | 40.0 | 125 | 110.5 | 144.8 | 0.958 |

*from Milosavljević *et al.* (2018)

small part of the rebar anchor adjacent to the coupler. Therefore, the total bearing area of the connector A_f , according to Fig. 9, is expressed as

$$A_f = l_{co} \cdot d_{co} + \Delta l_{co} \cdot d_a \quad (4)$$

where

l_{co} length of mechanical coupler
 d_{co} diameter of mechanical coupler
 Δl_{co} the activated length of rebar anchor
 d_a diameter of rebar anchor

The equivalent influence length for mechanical coupler $l_{f, eq}$, with constant diameter of mechanical coupler over the embedment depth d_{co} , can be approximated as

$$l_{f, eq} = A_f/d_{co} = l_{co} + \Delta l_{co} \cdot d_a/d_{co} \quad (5)$$

The activated length of rebar anchor Δl_{co} , was measured for each FE model in parametric study which failed in concrete edge failure mode or combined failure mode (CEF and

CEF/BSF in Table 5), as well as for FEM_A model which was initially calibrated to match the results of corresponding experimental push-out specimens, as described in Milosavljević *et al.* (2018). Values of $\Delta l_{co, FEM}$ are presented in Table 7. Based on the analysis of measured values, it was concluded that activated length of rebar anchor mostly depends on diameter of rebar anchor d_a and concrete compressive strength f_{cm} . The proposed equation for calculating length Δl_{co} is given in Eq. (6) and the comparison with numerical results is presented in Table 7. It is shown that the prediction equation Eq. (6) gives reasonably accurate results.

$$\Delta l_{co} = \frac{30}{f_{cm}^{0.38}} \cdot d_a^{0.5} \quad (6)$$

Substituting the Eq. (6) in Eq. (5) leads to the proposed method for calculating the equivalent influence length $l_{f, eq}$ of shear connectors with mechanical coupler, as shown in Eq. (7).

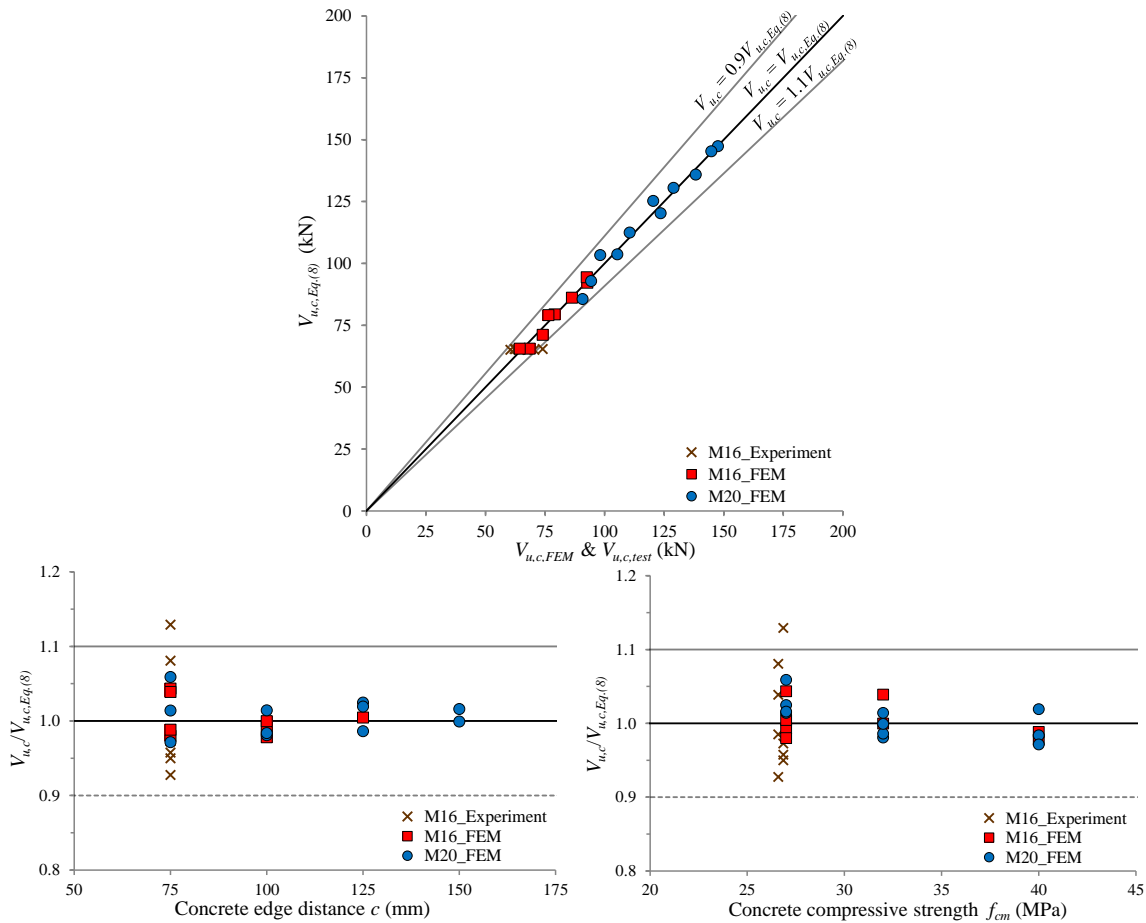


Fig. 10 Comparison of concrete edge breakout load: design method vs. test and FE results

$$l_{f,eq} = l_{co} + \frac{30}{f_{cm}^{0.38}} \cdot \frac{d_a^{1.5}}{d_{co}} \quad (7)$$

$$V_{u,c} = 47 \cdot \sqrt{f_{cm}} \cdot c^{2/3} \cdot d_{co} \cdot \left(\frac{l_{f,eq}}{12d_{co}} \right)^{0.3} \quad (8)$$

4.2.2 Concrete edge breakout resistance and validation vs. numerical and experimental results

The proposed method for calculating concrete edge breakout resistance of bolted shear connectors with mechanical coupler in this paper is based on the adjustment of the existing prediction model derived by Grosser (2012), by introducing equivalent influence length of the connector with variable diameter $l_{f,eq}$, as explained in previous section. Instead of the embedment depth l_f , the equivalent influence length of mechanical coupler $l_{f,eq}$ given by Eq. (7) is used to determine the influence of the connector’s stiffness ratio $l_{f,eq}/d_{co}$ on concrete edge breakout resistance, which is accounted for by factor $\psi_{l,V}$ in Eq. (2). It is shown that the values of stiffness ratio $l_{f,eq}/d_{co}$ for shear connectors with mechanical coupler considered in this paper are lower than 12 in all cases (see Table 7), hence the value of power law parameter x in Eq. (3) is adopted as $x = 0.3$. Finally, the proposed equation for calculating mean value of concrete edge breakout resistance is given as

In order to prove the applicability of the proposed method, values of concrete edge breakout load calculated according to Eq. (8), for different values of key parameters within the range considered in this paper and in Milosavljević *et al.* (2018), are compared to corresponding experimental and numerical results.

The experimental tests have shown that concrete edge breakout failure load does not represent the ultimate resistance of bolted shear connectors with mechanical coupler, since concrete breakout body in reinforced concrete members is limited to the concrete cover, as described in Milosavljević *et al.* (2018). Instead, it was identified as stiffness reduction (change of slope) on force-slip curves, at around 70% of the ultimate connection resistance. The measured values of vertical force and slip at the attainment of concrete edge breakout failure are given in Table 8.

Concrete edge breakout load on FE models was identified at the point of total propagation of cracks from the connector towards the concrete edge, which represents the point where concrete breakout body is fully developed. The values of concrete edge breakout load obtained for FE models included in parametric study and Milosavljević *et al.*

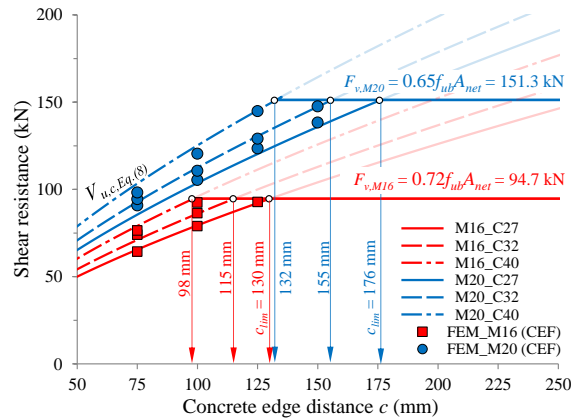


Fig. 11 Derivation of minimum concrete edge distance to avoid concrete edge failure

(2018) are presented in Table 9. It can be concluded that the ratio $V_{u,c,FEM}/P_{ult,FEM}$ for FE models FEM_A and M16_C27_D75 are similar to the same ratio of corresponding test specimens (Table 8). Furthermore, it should be noted that this ratio increases with increasing concrete edge distance and/or concrete strength. FE models with the values of $V_{u,c,FEM}/P_{ult,FEM}$ ratio higher than 0.90, have failed in combined failure mode (designated as CEF/BSF in Table 5).

The comparison of the results of FE parametric study, experimental and FE analyses conducted in Milosavljević *et al.* (2018) with values of concrete edge breakout load according to the proposed calculation prediction given by Eq. (8) is presented in Fig. 10. The comparison shows good correlation with test and FE results for all key parameters in range considered in this paper. The average $V_{u,c}/V_{u,c,Eq.(8)}$ ratio, which includes both FEM-to-predicted and test-to-predicted ratios, is 1.01 with standard deviation $s_x = 0.04$ and coefficient of variation $V_x = 4.37\%$.

4.3 Recommendations for minimum edge distance to avoid concrete edge breakout failure

As explained in previous sections, the combination of small concrete edge distance, low concrete strength and high anchor shear strength can lead to a premature concrete edge failure of anchors as well as bolted connectors with mechanical coupler. For anchors, different design guides, reports and codes give recommendations for limiting values of edge distance c_{lim} , as a function of effective depth or anchor diameter, large enough to assure that concrete edge failure will be avoided. Limiting values c_{lim} are defined by varying concrete edge distance of the anchor and by comparing corresponding concrete edge failure load to the shear resistance of the anchor. Usually, the recommendations for c_{lim} are obtained for the so-called “worst case scenario” i.e. for the maximum diameter and strength of the anchor combined with the lowest concrete class allowed by codes or approvals.

For anchor groups of 4 or less anchors, CEB-FIP (2011) permits to omit the check of concrete edge failure if the edge distance is greater than $60d_{nom}$ and $10h_{ef}$ in all

directions. Grosser (2012) conducted aforementioned analysis for mean and design values of shear resistances in concrete edge breakout failure ($V_{u,c}$ and $0.75V_{u,c}/1.5$, respectively) and bolt shear failure ($V_{u,s}$ and $0.8V_{u,s}/1.25$, respectively), with assumption of both cracked and uncracked concrete ($k_{cr} = 0.7k_{uncr}$). Anchor diameter $d_{nom} = 30$ mm, steel strength $f_u = 800$ MPa and concrete strength $f_{cm} = 20$ MPa were used. In case of design resistances in cracked concrete, the obtained concrete edge distance c_{lim} was equal to $c_{lim} = \max(30d_{nom}, 5h_{ef})$, while in case of mean resistances in uncracked concrete (test conditions) it was equal to $c_{lim} = \max(14d_{nom}, 2.5h_{ef})$.

The derivation of minimum concrete edge distance to avoid concrete edge failure of bolted connector with mechanical coupler is not straightforward as in case of anchors with constant diameter. While shear resistance of connectors with mechanical coupler is governed by shear capacity of bolts (BSF mode) i.e., diameter and tensile strength, concrete edge failure resistance (CEF mode) is determined by combination of concrete strength, diameter and length of mechanical coupler and diameter of rebar anchor embedded in concrete, as explained in Section 4.2. Fig. 11 shows the obtained values of edge distances at intersection of concrete edge breakout load and shear strength of bolts. Concrete strengths and bolt diameters with corresponding dimensions of mechanical coupler are varied within the range used in parametric study in Section 3. It is shown that the value of minimum required concrete edge distance to avoid edge breakout failure increases approximately by 30% in case of lower concrete strengths or larger bolt diameter. Based on the concept described above, limiting values of concrete edge distance for M16 and M20 bolts were adopted as $c_{lim} = 130$ mm ($c_{lim}/d_{co} = 5.9$) and $c_{lim} = 176$ mm ($c_{lim}/d_{co} = 6.5$), respectively. In case of concrete strength $f_{cm} = 20$ MPa and M20 bolts ($d_{co} = 27$ mm), the ratio of limiting concrete edge distance to coupler diameter would be $c_{lim}/d_{co} = 8.1$ which is lower than the same ratio obtained by Grosser (2012) for anchor diameter $d_{nom} = 30$ mm. The apparent reason is lower shear strength of M20 bolts (i.e., lower BSF-to-CEF resistance ratio) compared to the anchor with diameter of $d_{nom} = 30$ mm.

5. Conclusions

This paper presents the analysis of the behaviour of bolted shear connectors with mechanical coupler in steel-concrete composite connections, based on FE simulation of push-out tests conducted in Abaqus software and experimental test results. Complex contact interactions and nonlinear properties and damage of concrete and steel materials were incorporated in FE models, which have been validated by push-out tests. FE parametric study was conducted in order to investigate the effect of most influencing parameters on the behaviour of bolted shear connectors with mechanical coupler: concrete edge distance, concrete strength and bolt diameter i.e. coupler diameter. For considered range of key parameters, the most important conclusions are:

- Bolted shear connection with mechanical coupler can exhibit only two failure modes – concrete edge breakout failure and bolt shear failure, while pullout and pryout failures are eliminated by long rebar anchor. The combination of small edge distance and low concrete strength leads to premature concrete edge breakout failure, regardless of bolt diameter.
- Concrete edge failure occurs at connection slip in range of 1-2 mm. However, breakout of concrete edge is limited only to the concrete cover and further increase of shear load is possible. At ultimate, concrete failure results in more ductile failure mode than shear failure of bolts, with up to 83% and 107% larger ultimate slip for M16 and M20 bolts, respectively. Furthermore, the increase of bolt diameter from M16 to M20 increases the connection slip from 10% to 50%, depending on the type of failure mode.
- The results showed that ultimate resistance is increased by approximately 60% with increase of bolt diameter from M16 to M20 for the same concrete edge distance.
- The reduction of concrete edge distance causes the change of failure mode from bolt shear failure to concrete edge failure, with increase of shear resistance up to 10% due to rotation of connector's axis and catenary effects. This increase of shear resistance results from efficient anchorage of bolted shear connector with mechanical coupler and long rebar anchor in reinforced concrete members.
- In case of bolt shear failure, shear resistance factor i.e., shear-to-tensile strength ratio, is equal to 0.72 for M16 bolts and 0.65 for M20 bolts.

Based on FE results, the model for hand calculation of concrete edge breakout resistance of bolted shear connectors with mechanical coupler is proposed. The proposed model takes into account all relevant parameters: concrete edge distance, concrete strength and connector's stiffness. The effect of variable diameter over the embedment depth on concrete breakout resistance was considered by defining the equivalent influence length of the connector. The validity of the proposed equation was confirmed by very good agreement between the proposed equation and test results. The recommendations for

minimum edge distance to avoid concrete edge failure are given.

Acknowledgments

The research described in this paper was supported by the Serbian Ministry of Education, Science and Technological Development through the TR-36048 project.

References

- Ataei, A., Bradford, M. and Liu, X. (2016), "Experimental study of composite beams having a precast geopolymer concrete slab and deconstructable bolted shear connectors", *Eng. Struct.*, **114**, 1-13. <https://doi.org/10.1016/j.engstruct.2015.10.041>
- Brambilla, G., Lavagna, M., Vasdravellis, G. and Castiglioni, C.A. (2019), "Environmental benefits arising from demountable steel-concrete composite floor systems in buildings", *Resources, Conservation & Recycling*, **141**, 133-142. <https://doi.org/10.1016/j.resconrec.2018.10.014>
- CEB-FIP (2011), "Design of Anchorages in Concrete (fib Bulletin 58)", International Federation for Structural Concrete (fib); Lausanne, Switzerland.
- Dallam L.N. (1968), "High strength bolts shear connectors – pushout tests", *ACI J. Proc.*, **65**(9):767-769
- Dedic, D.J. and Klaiber, W.F. (1984), "High-strength bolts as shear connectors in rehabilitation work", *Concr. Int.*, **6**(7), 41-46.
- Dai, X.H., Lam, D. and Saveri, E. (2015), "Effect of concrete strength and stud collar size to shear capacity of demountable shear connectors", *J. Struct. Eng.*, **141**(11), 04015025:1-10. [https://doi.org/10.1061/\(ASCE\)ST.1943-541X.0001267](https://doi.org/10.1061/(ASCE)ST.1943-541X.0001267).
- Eurocode 2 (2004), Design of concrete structures. Part 1.1: General rules and rules for buildings, European Committee for Standardization (CEN); Brussels, Belgium.
- Eurocode 3 (2005), Design of steel structures. Part 1.8: Design of joints, European Committee for Standardization (CEN); Brussels, Belgium.
- Eurocode 4 (2004), Design of composite steel and concrete structures. Part 1.1: General rules and rules for buildings, European Committee for Standardization (CEN); Brussels, Belgium.
- Hawkins, N. (1987), "Strength in shear and tension of cast-in-place anchor bolts", *Anchorage Concr.*, SP-103, 233-255.
- Guezouli, S., Lachal, A. and Nguyen, Q.H. (2013), "Numerical investigation of internal force transfer mechanism in push-out tests", *Eng. Struct.*, **52**, 140-152. <http://dx.doi.org/10.1016/j.engstruct.2013.02.021>
- Grosser, P. (2012), "Load-bearing behavior and design of anchorages subjected to shear and torsion loading in uncracked concrete", Ph.D. Dissertation; Institut für Werkstoffe im Bauwesen der Universität Stuttgart, Stuttgart, Germany.
- Kwon, G. (2008), "Strengthening existing steel bridge girders by the use of post-installed shear connectors", Ph.D. Dissertation; The University of Texas at Austin, Austin, Texas, USA.
- Lam, D., Dai, X., Ashour, A. and Rahman, N. (2017), "Recent research on composite beams with demountable shear connectors", *Steel Constr. Des. Res.*, **10**(2), 125-134. <https://doi.org/10.1002/stco.201710016>.
- Lee, M. and Bradford, M.A. (2013), "Sustainable composite beam behaviour with deconstructable bolted shear connectors", *Proceedings of the Composite Construction in Steel and Concrete VII*, Palm Cove, Australia, July. <https://doi.org/10.1061/9780784479735.034>.

- Liu, X., Bradford, M. and Lee, M. (2014), "Behavior of High-Strength Friction-Grip Bolted Shear Connectors in Sustainable Composite Beams", *J. Struct. Eng.*, **141**(6), 04014149:1-12. [https://doi.org/10.1061/\(ASCE\)ST.1943-541X.0001090](https://doi.org/10.1061/(ASCE)ST.1943-541X.0001090).
- Marshall, W.T., Nelson, H.M. and Banerjee, H.K. (1971), "An experimental study of the use of high-strength friction-grip bolts as shear connectors in composite beams", *Struct. Eng.*, **49**(4), 171-178.
- Milosavljević, B. (2013), "Theoretical and experimental research of the behaviour of reinforced concrete and steel element connection by rebar couplers", Ph.D. Dissertation; University of Belgrade, Belgrade, Serbia.
- Milosavljević, B., Milićević, I., Pavlović, M. and Spremić, M. (2018), "Static behaviour of bolted shear connectors with mechanical coupler embedded in concrete", *Steel Compos. Struct.*, **29**(2), 257-272. <https://doi.org/10.12989/scs.2018.29.2.257>.
- Oehlers, D.J. (1980), "Stud shear connectors for composite beams", Ph.D. Dissertation; University of Warwick, Coventry CV4 7AL, UK.
- Okada J., Teruhiko, Y. and Lebet, J.P. (2006), "A study of the grouped arrangements of stud connectors on shear strength behaviour", *Struct. Eng. Earthq. Eng.*, **23**(1), 75-89. <https://doi.org/10.2208/jscseee.23.75>.
- Ollgaard, J.G., Slutter, R.G. and Fisher, J.W. (1971), "Shear strength of stud connectors in lightweight and normalweight concrete", *Eng. J. Amer. Inst. Steel Constr.*, **8**(2), 55-64.
- Pallarés, L. and Hajjar, J.F. (2010), "Headed steel stud anchors in composite structures, part I: shear", *J. Constr. Steel Res.*, **66**(2), 198-212. <https://doi.org/10.1016/j.jcsr.2009.08.009>.
- Pathirana, S.W., Uy, B., Mirza, O. and Zhu, X. (2016), "Bolted and welded connectors for rehabilitation of composite beams", *J. Constr. Steel Res.*, **125**, 61-73. <https://doi.org/10.1016/j.jcsr.2016.06.003>.
- Pavlović M., Marković Z., Veljković M. and Budjevac D. (2013), "Bolted shear connectors vs. headed studs behaviour in push-out tests", *J. Constr. Steel Res.*, **88**, 134-149. <https://doi.org/10.1016/j.jcsr.2013.05.003>
- Pavlović, M. (2014), "Resistance of Bolted Shear Connectors in Prefabricated Steel-Concrete Composite Decks, Ph.D. Dissertation; University of Belgrade, Belgrade, Serbia.
- Pavlović, M. and Veljković, M. (2017), "FE validation of push-out tests", *Steel Constr. Des. Res.*, **10**(2), 135-144. <https://doi.org/10.1002/stco.201710017>.
- Schaap, B.A. (2004): Methods to develop composite action in non-composite bridge floor systems: Part I. MSc thesis, The University of Texas, Austin, Texas.
- Spremić, M., Marković, Z., Veljković, M. and Budjevac, D. (2013), "Push-out experiments of headed shear studs in group arrangements", *Adv. Steel Constr.*, **9**(2), 139-160. <http://dx.doi.org/10.18057/IJASC.2013.9.2.4>.
- Spremić, M., Marković, Z. and Veljković, M. (2017), "Recommendations for the design of grouped headed studs", *Steel Constr. Des. Res.*, **10**(2), 145-153. <https://doi.org/10.1002/stco.201710018>.
- Spremić, M., Pavlović, M., Marković, Z., Veljković, M. and Budjevac, D. (2018), "FE validation of the equivalent diameter calculation model for grouped headed studs", *Steel Compos. Struct.*, **26**(3), 375-386. <https://doi.org/10.12989/scs.2018.26.3.375>.
- Xu, C., Sugiura, K., Wu, C. and Su, Q. (2012), "Parametrical static analysis on group studs with typical push-out tests", *J. Constr. Steel Res.*, **72**, 84-96.
- Xue, D., Liu, Y., Yu, Z. and He, J. (2012), "Static behavior of multi-stud shear connectors for steel-concrete composite bridge", *J. Constr. Steel Res.*, **74**, 1-7. <https://doi.org/10.1016/j.jcsr.2011.09.017>.
- Yang, F., Liu, Y., Jiang, Z. and Xin, H. (2018), "Shear performance of a novel demountable steel-concrete bolted connector under static push-out tests", *Eng. Struct.*, **160**, 133-146. <https://doi.org/10.1016/j.engstruct.2018.01.005>.
- Yu-Hang, W., Jie, Y., Jie-Peng, L. and Chen, Y.F. (2019), "Shear behavior of shear stud groups in precast concrete decks", *Eng. Struct.*, **187**, 73-84. <https://doi.org/10.1016/j.engstruct.2019.02.002>.

DL